

Supporting Information for:

Tyrosine, cysteine, and proton coupled electron transfer in a ribonucleotide
reductase-inspired beta hairpin maquette

Tyler G. McCaslin,^{a,b} Cynthia V. Pagba,^{a,b} Hyea Hwang,^c James C. Gumbart,^{a,b,d}
San-Hui Chi,^{a,e} Joseph W. Perry,^{a,e} and Bridgette A. Barry^{a,b*}

^aSchool of Chemistry and Biochemistry, ^bThe Parker H. Petit Institute of
Bioengineering and Bioscience, ^cSchool of Materials Science and Engineering,
^dSchool of Physics, and ^eCenter of Organic Photonic and Electronics
Georgia Institute of Technology, Atlanta, GA 30332, U. S. A.

Table of Contents

Description of Materials and Methods

Table S1. Charge on Y5 and C14 as a function of pH

Table S2. Table of biexponential fits to the TRAS data

References

Figure S1. Circular dichroism (CD) and thermal melting of Peptide A and Peptide O

Figure S2. CD of Peptide O in the presence and absence of dithiothreitol (DTT)

Figure S3. Schematics of Peptide O charge as a function of pH and experimental protocols

Figure S4. Electron paramagnetic resonance (EPR) spectra of Peptide O

Figure S5. Molecular dynamics simulations of Peptide O in various charge states

Figure S6. Electrochemical and UV-Vis titrations of Peptide O

Figure S7. Transient absorption spectra (TRAS) of tyrosinate, Peptide A, Peptide C, and Peptide O at pD 11

Figure S8. Transient absorption spectra (TRAS) of tyrosine, Peptide A, Peptide C, and Peptide O at pD 9

Figure S9. Decay kinetics after a 280 nm femtosecond flash as derived from tyrosine/tyrosinate, Peptide A, Peptide C, and Peptide O at pD 9 and 11

Materials and Methods

Chemicals and Peptide Samples. Boric acid (99% purity), HEPES (4-(2-hydroxyethyl)-1-piperazineethanesulfonic acid, 99.5 %), sodium hydroxide (99.5 %) and tyrosine (99.9%) were purchased from Sigma (St. Louis, MO). DL-dithiothreitol (DTT, 99.5%) was purchased from MP Biomedicals (Santa Ana, CA). Deuterium oxide (D₂O, 99.9 %) and sodium deuterioxide (NaOD, 99.5%) were purchased from Cambridge Isotope Laboratories (Andover, MA). Peptide A (IMDRYRVRNGDRIHIRLR), Peptide C (IMDRYRVRNGDRICaIRLR), and Peptide O (IMDRYRVRNGDRICIRLR) were synthesized by solid state synthesis and were obtained from Genscript (Piscataway, NJ; >95% purity).^{1, 2} Because Peptide O was sparingly soluble in H₂O buffers at the high concentrations required for TRAS, TRAS experiments were conducted in D₂O containing buffers, which improved solubility. The pD is reported as the uncorrected meter reading.³

Circular Dichroism (CD). CD spectra of 100 μM samples were collected from 250 nm to 193 nm in a 1 mm quartz cuvette using a Jasco J-810 CD spectropolarimeter, equipped with a Peltier-type cell.^{2, 4, 5} Twenty-four accumulations per scan were averaged in three independent measurements for each of the temperature conditions. Parameters used were: sensitivity, 100 mdeg; data pitch, 2 nm; scan speed, 50 nm/min; response time, 1 s; bandwidth, 1 nm.

Electron paramagnetic resonance (EPR) Spectroscopy. EPR spectroscopy was performed using prior methods.^{1, 4, 5} Spectra were recorded on a Bruker (Billerica, MA) EMX spectrometer equipped with a Bruker ER 4102ST cavity and Bruker ER 4131VT temperature control unit set to 160 K. Field sweep spectra were acquired following fifty UV laser flashes. Spectrometer parameters: microwave frequency, 9.4 GHz; microwave power, 600 μW; modulation amplitude, 1 G; modulation frequency, 100 kHz; scan time, 168 s; number of scans,

4; time constant, 655 ms. Radicals were generated at 160 K using 50 flashes at 266 nm (10 mJ) by the fourth harmonic of a Nd-YAG laser (Continuum Surelite III, Santa Clara, CA). Laser energy was approximately 40 mJ per pulse of a beam diameter of approximately 1 cm. Experiments were conducted in triplicate.

Differential Pulse Voltammetry (DPV). DPV was performed by a method previously described^{1, 2} in a three-electrode electrochemical cell with a 3 mm glassy carbon working electrode, Ag/AgCl (1 M KCl) reference electrode, and platinum wire counter electrode using a Princeton Applied Research 273A potentiostat. Ru(NH₃)₆Cl₃ (200 μM in 1 M KCl) was used as an electrochemical standard before each set of measurements and the peak potential was measured to be -200 mV vs Ag/AgCl, as expected. Data were averaged from three independent measurements and smoothed using CorrView3 (Scribner, Southern Pines, NC). Measured potentials are the centroid of the electrochemical peak converted from vs Ag/AgCl ($E = 0.22$ V vs NHE) to vs NHE. DPV parameters: potential range, -0.5 - +1.5 V vs reference; scan speed, 32 mV/s; differential pulse amplitude, 25 mV. Buffer contained 100 μM peptide, 200 mM KCl, and 5 mM MES (pH 6 - 6.5), HEPES (pH 7 - pH 8), or borate/NaOH (pH 8.5 - pH 11). Samples were purged with argon prior to and during measurement.

UV absorbance spectroscopy. UV absorbance was measured using a Shimadzu UV-1700 spectrophotometer (Kyoto, Japan) and 1 cm path length quartz cuvettes. Data were measured in triplicate and averaged. Buffer contained 100 μM peptide, 200 mM KCl, and 5 mM MES (pH 6 - 6.5), HEPES (pH 7 - pH 8), or borate/NaOH (pH 8.5 - pH 11). Tyrosinate concentration was calculated from Beer's Law using the extinction coefficients for Peptide A (1550 L mol⁻¹ cm⁻¹) and Peptide O (1540 L mol⁻¹ cm⁻¹) and the difference in absorbance of A₂₉₅ and A₃₃₀. The extinction coefficients of Peptide A and Peptide O are similar to that of tyrosine.⁶

Time resolved absorption spectroscopy (TRAS). The TRAS system consists of a regeneratively amplified titanium sapphire laser (Solstice, Spectra-Physics, 800-nm) and a computer-controlled optical parametric amplifier (OPA) (Spectra-Physics, TOPAS), as previously described.^{5, 7-9} The 280-nm photolysis pulse was produced using OPA and a white-light continuum (WLC) probe beam with 350-750 nm spectral range was generated from the 800-nm amplified beam. The sample solutions had an OD₂₈₀ of 0.25–0.50 in 2 mm path-length cuvettes. They were stirred throughout data acquisition to prevent photodegradation. Triplet formation is not expected in oxygenated samples.¹⁰ To verify the integrity of the sample, steady state absorption spectra were recorded before and after the ultrafast measurements on a Shimadzu UV-3101PC. TRAS were acquired with a pump-white light continuum probe spectroscopy system (Ultrafast Systems, Helios).⁷ The system consists of a regeneratively amplified titanium sapphire laser (Solstice, Spectra-Physics, 800-nm, 3.7-W average power, 100-fs pulse width, 1-KHz repetition rate) and a computer-controlled optical parametric amplifier (OPA) (Spectra-Physics, TOPAS, wavelength range: 266-2600 nm, pulse width: ~75 fs HW_{1/e}) pumped by the amplified laser. The 280-nm photolysis pulse was generated using the fourth-harmonic output of the OPA. A white-light continuum (WLC) probe beam with 350-750 nm spectral range was generated by focusing less than 5% of the 800-nm amplified beam into a CaF₂ crystal. The probe signal was collected using a fiber optic cable coupled to a spectrometer with a multichannel CMOS (spectral range 300-900 nm) sensor. The maximum time delay was 3.2 ns. The pump beam was chopped at 500 Hz to obtain the WLC spectrum without pump and alternately with the 280-nm pump. These data were used to calculate the transient spectra, represented as a change in optical density or absorbance units (AU). Each transient spectrum at a given time delay was averaged for 4 seconds. A chirp correction function for the WLC probe

was determined using the coherent artifact of the organic solvent, tetrahydrofuran, and was applied to all transient spectra.¹¹ The optical path length of the quartz cuvette was 2 mm. The excitation pulse energy was 2-3 μJ . The averaged beam waist ($\text{HW}_{1/e}$) was ~ 160 μm for the pump and ~ 80 μm for the WLC. The solutions had an OD_{280} of 0.25–0.50 in 2 mm path-length cuvettes and were stirred throughout data acquisition to prevent photoinduced degradation. The tyrosyl radical was not generated at pH values less than 9. To verify the integrity of the sample, steady state absorption spectra were recorded before and after the ultrafast measurements on a Shimadzu UV-3101PC.

Molecular dynamics simulations. The three-dimensional minimized structure of Peptide A, which was used in the previous work,¹² was used as the initial structure. Peptide O was built by replacing H14 with cysteine (C14). We considered three charge states Peptide O-YH (tyrosine), Peptide O-Y⁻ (deprotonated tyrosine, tyrosinate), and Peptide O-Y \cdot (neutral tyrosyl radical) based on the charge state of Y5. When tyrosine is protonated (O-YH) at pD 9 or in a neutral radical state (O-Y \cdot), the cysteine is present in both its protonated and deprotonated forms. Therefore, we built two more systems in which C14 was deprotonated (YH-deC and Y \cdot -deC). When tyrosine is deprotonated at pH 11 (O-Y⁻), the cysteine is always deprotonated as well. In total, we built 5 systems, summarized in Table S1.

The initial size of the periodic box was $55 \times 55 \times 51$ \AA^3 . All peptide models were solvated with TIP3P water and neutralized with 150 mM NaCl. Each system was minimized for 1000 steps, after which the solvent was equilibrated while the peptide backbone was restrained for 2 ns. All analysis was done on subsequent 200-ns unrestrained production runs. Molecular dynamics simulations were carried out with NAMD¹³ and the CHARMM36 force field¹⁴ was used. The atomic charges for the neutral tyrosyl radical used here were optimized previously.¹²

The temperature was maintained at 300 K using Langevin dynamics and the pressure was kept at 1 atm using the Langevin piston method. A 2-fs time step was employed. Bonded terms were evaluated every time step, and nonbonded terms and long-range electrostatic interactions were updated every 2 fs and 4 fs, respectively. Long-range electrostatic interactions were calculated using the particle-mesh Ewald method.¹⁵ van der Waals interactions were cut off at 12 Å, and a switching function was used beginning at 10 Å. System setup and analysis were performed using VMD.¹⁶

Table S1. Molecular dynamics simulation models and corresponding protonation state as a function of simulated pH

Name	Y5	C14	pH
YH-C	protonated	protonated	9
YH-deC	protonated	deprotonated	9
Y ⁻ -deC	deprotonated	deprotonated	11
Y [•] -C	tyrosyl radical	protonated	9
Y [•] -deC	tyrosyl radical	deprotonated	9

Table S2. Kinetic parameters obtained from double exponential^a fits to TRAS of tyrosine,^b Peptide A,^b Peptide C,^b and Peptide O

	τ_1	A ₁ (%)	τ_2	A ₂ (%)	y ₀ (%)	χ^2
pD 9						
Tyrosine						
410 nm	22 ± 8	0.12 (13)	832 ± 54	0.23 (25)	0.56 (62)	0.0230
520 nm	23 ± 7	0.15 (16)	684 ± 36	0.30 (32)	0.48 (52)	0.0223
650 nm	30 ± 10	0.10 (11)	869 ± 35	0.27 (29)	0.56 (60)	0.0115
Peptide A						
410 nm	14 ± 2	0.28 (33)	703 ± 41	0.28 (33)	0.29 (34)	0.0282
520 nm	18 ± 2	0.28 (34)	576 ± 27	0.34 (42)	0.20 (24)	0.0208
650 nm	49 ± 9	0.20 (22)	626 ± 18	0.34 (38)	0.36 (40)	0.0203
Peptide C						
410 nm	13 ± 4	0.10 (11)	598 ± 24	0.31 (35)	0.48 (54)	0.0139
520 nm	30 ± 7	0.15 (17)	652 ± 22	0.36 (40)	0.38 (43)	0.0120
650 nm	40 ± 8	0.16 (18)	695 ± 22	0.28 (31)	0.46 (51)	0.0111
Peptide O						
410 nm	168 ± 34	0.12 (16)	1027 ± 24	0.40 (53)	0.24 (31)	0.0189
520 nm	95 ± 16	0.20 (25)	1005 ± 26	0.40 (49)	0.21 (26)	0.0205
650 nm	92 ± 15	0.19 (23)	968 ± 30	0.33 (39)	0.32 (38)	0.0193
pD 11						
Tyrosinate						
410 nm	81 ± 6	0.30 (32)	724 ± 95	0.06 (6)	0.58 (62)	0.0124
520 nm	73 ± 3	0.45 (50)	792 ± 41	0.11 (12)	0.34 (38)	0.0084
650 nm	113 ± 7	0.28 (29)	858 ± 37	0.14 (14)	0.56 (57)	0.0095
Peptide A						
410 nm	101 ± 6	0.36 (51)	1081 ± 94	0.08 (11)	0.26 (37)	0.0140
520 nm	76 ± 4	0.42 (56)	858 ± 72	0.13 (17)	0.20 (27)	0.0064
650 nm	90 ± 8	0.34 (37)	1137 ± 78	0.21 (23)	0.37 (42)	0.0116
Peptide C						
410 nm	72 ± 7	0.36 (51)	1072 ± 120	0.09 (13)	0.26 (37)	0.0262
520 nm	73 ± 3	0.48 (63)	750 ± 64	0.08 (11)	0.20 (26)	0.0128
650 nm	94 ± 5	0.39 (42)	1095 ± 56	0.12 (13)	0.41 (45)	0.0104
Peptide O						
410 nm	105 ± 7	0.37 (53)	947 ± 91	0.09 (13)	0.24 (34)	0.0190
520 nm	56 ± 3	0.30 (42)	352 ± 11	0.21 (29)	0.21 (29)	0.0052
650 nm	78 ± 5	0.29 (34)	448 ± 15	0.20 (23)	0.37 (43)	0.0065

^a $y = y_0 + A_1 \exp\{-(x-x_0)/\tau_1\} + A_2 \exp\{-(x-x_0)/\tau_2\}$; A = Amplitude, τ = time constant (ps), $x_0 = 20$ ps. The transients were normalized with respect to the maximum absorbance in each averaged data, which occurs ~ 3-4 ps at 410 and 520 nm and ~ 10-15 ps at 650 nm, before fitting with Igor Pro 6.34A (Wavemetrics Inc., Lake Oswego, OR).^bKinetic parameters for tyrosine and Peptide A in H₂O were obtained from previous work.⁹

References

1. R. Sibert, M. Josowicz, F. Porcelli, G. Veglia, K. Range and B. A. Barry, *J. Am. Chem. Soc.*, 2007, **129**, 4393-4400.
2. R. S. Sibert, M. Josowicz and B. A. Barry, *ACS Chem. Biol.*, 2010, **5**, 1157-1168.
3. D. L. Jenson and B. A. Barry, *J. Am. Chem. Soc.*, 2009, **131**, 10567-10573.
4. C. V. Pagba, T. G. McCaslin, G. Veglia, F. Porcelli, J. Yohannan, Z. Guo, M. McDaniel and B. A. Barry, *Nat. Commun.*, 2015, **10010**.
5. T. G. McCaslin, C. V. Pagba, S.-H. Chi, H. J. Hwang, J. C. Gumbart, J. W. Perry, C. Olivieri, F. Porcelli, G. Veglia, Z. Guo, M. McDaniel and B. A. Barry, *J. Phys. Chem. B*, 2019, **123**, 2780-2791.
6. D. B. Wetlaufer, J. T. Edsall and B. R. Hollingworth, *J. Biol. Chem.*, 1958, **233**, 1421-1428.
7. A. F. Chaudhry, M. Verma, M. T. Morgan, M. M. Henary, N. Siegel, J. M. Hales, J. W. Perry and C. J. Fahrni, *J. Am. Chem. Soc.*, 2009, **132**, 737-747.
8. C. V. Pagba, S. H. Chi, J. Perry and B. A. Barry, *J. Phys. Chem. B*, 2015, **119**, 2726-2736.
9. C. V. Pagba, T. G. McCaslin, S. H. Chi, J. W. Perry and B. A. Barry, *J. Phys. Chem. B*, 2016, **120**, 1259-1272.
10. D. V. Bent and E. Hayon, *J. Am. Chem. Soc.*, 1975, **97**, 2599-2619.
11. S. Kovalenko, A. Dobryakov, J. Ruthmann and N. Ernsting, *Phys. Rev. A*, 1999, **59**, 2369.

12. H. Hwang, T. G. McCaslin, A. Hazel, C. V. Pagba, C. M. Nevin, A. Pavlova, B. A. Barry and J. C. Gumbart, *J. Phys. Chem. B*, 2017, **121**, 3536-3545.
13. J. C. Phillips, R. Braun, W. Wang, J. Gumbart, E. Tajkhorshid, E. Villa, C. Chipot, R. D. Skeel, L. Kale and K. Schulten, *J. Comput. Chem.*, 2005, **26**, 1781-1802.
14. R. B. Best, X. Zhu, J. Shim, P. E. Lopes, J. Mittal, M. Feig and A. D. MacKerell Jr, *J. Chem. Theor. Comput.*, 2012, **8**, 3257-3273.
15. T. Darden, D. York and L. Pedersen, *J. Chem. Phys.*, 1993, **98**, 10089-10092.
16. W. Humphrey, A. Dalke and K. Schulten, *J. Mol. Graph.*, 1996, **14**, 33-38.

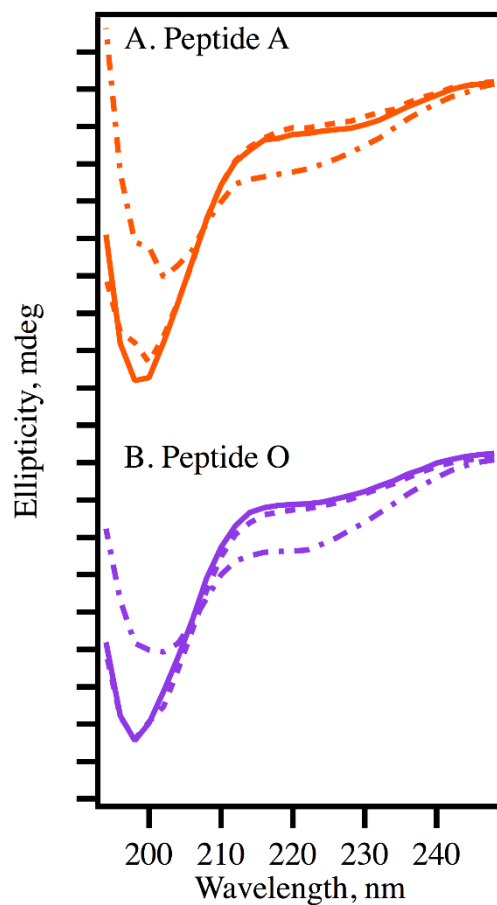


Figure S1. CD spectra derived from Peptide A (A, orange) and Peptide O (B, violet). The spectra were obtained at 20°C (solid line, pre-melt), 80°C (dot-dashed line), and at 20°C (dashed line, post-melt). The analyte concentration was 100 μ M, and the buffer contained 5 mM HEPES, pH 7.5. The spectra were averaged from three independent measurements. The tick marks denote 2 mdeg.

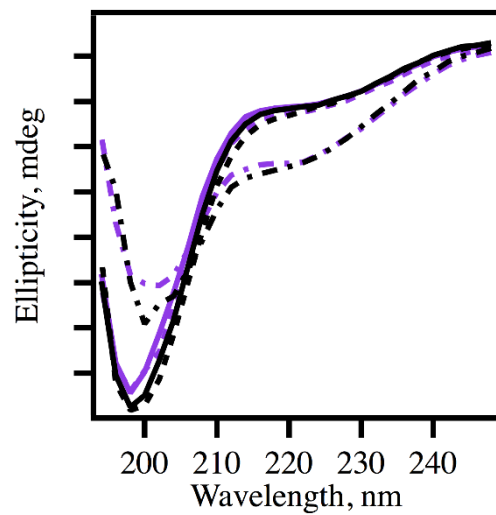


Figure S2. CD spectra of Peptide O (purple, reproduced from Figure S1 for comparison) and Peptide O + DTT (black). The spectra were obtained at 20°C (solid line, pre-melt), 80°C (dot-dashed line), and at 20°C (dashed line, post-melt). The peptide concentration was 100 μM , the DTT concentration was 200 μM , and the buffer contained 5 mM HEPES, pH 7.5. The spectra were averaged from three independent measurements. The tick marks denote 2 mdeg.

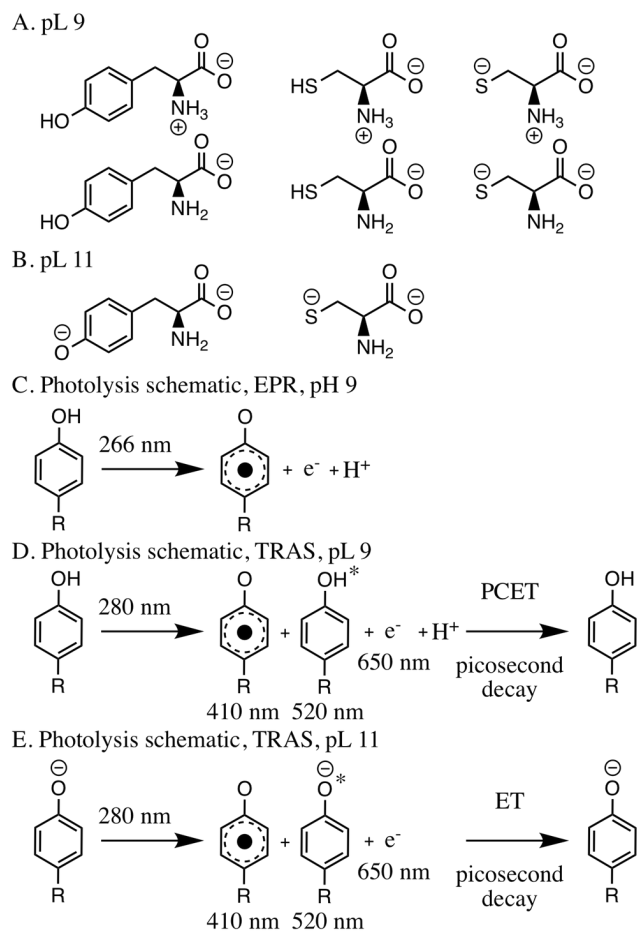


Figure S3. Scheme of protonation states of tyrosine and cysteine at pL 9 (A) and pL 11 (B). Scheme of UV photolysis in EPR experiments (C). Scheme of TRAS photolysis at pL 9 (D) and pL 11 (E).

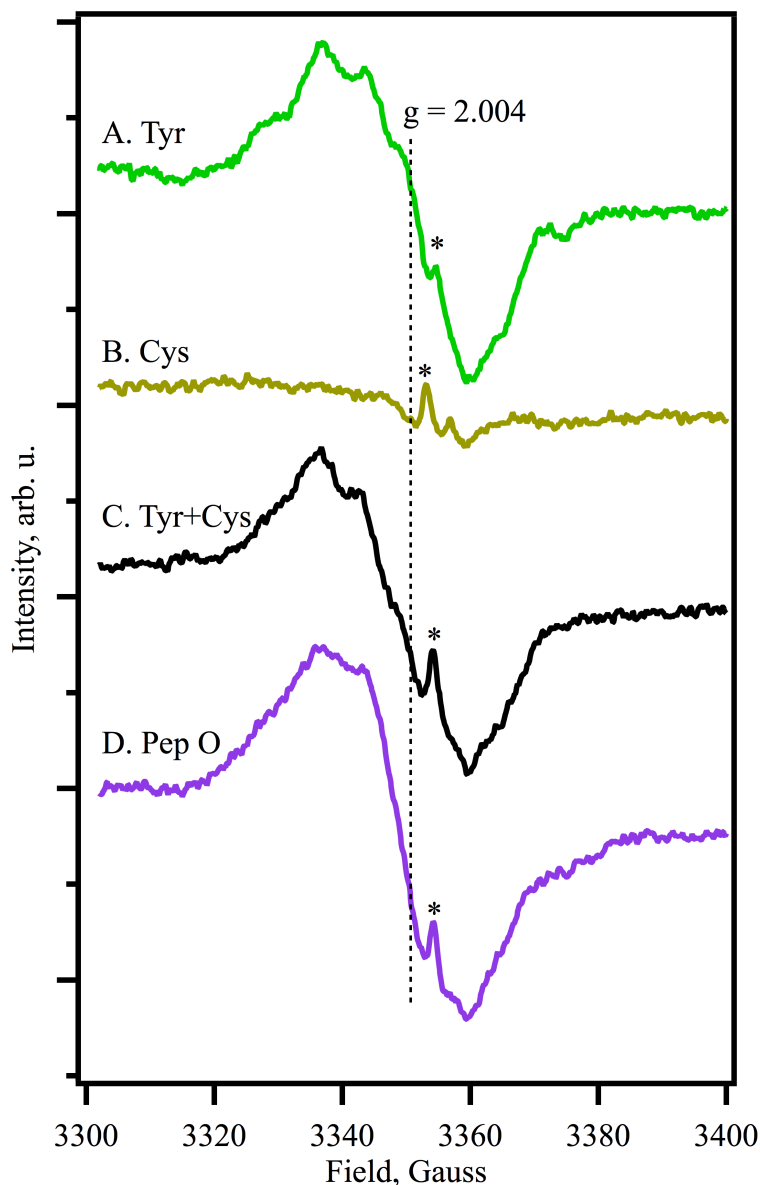


Figure S4. EPR spectra of tyrosine, cysteine, an equimolar tyrosine cysteine mixture, and Peptide O at pH 9 following UV photolysis at 160 k. X-band EPR spectra of tyrosine (A, green), cysteine (B, gold), tyrosine + cysteine solution (C, black), and Peptide O (D, purple). The analyte concentration was 250 μM , and the buffer contained 5 mM borate, pH 9. The data were averaged from three independent measurements and normalized to A_{366} . The tick marks denote 1000 units. The asterisk marks a small signal from the quartz EPR tube.

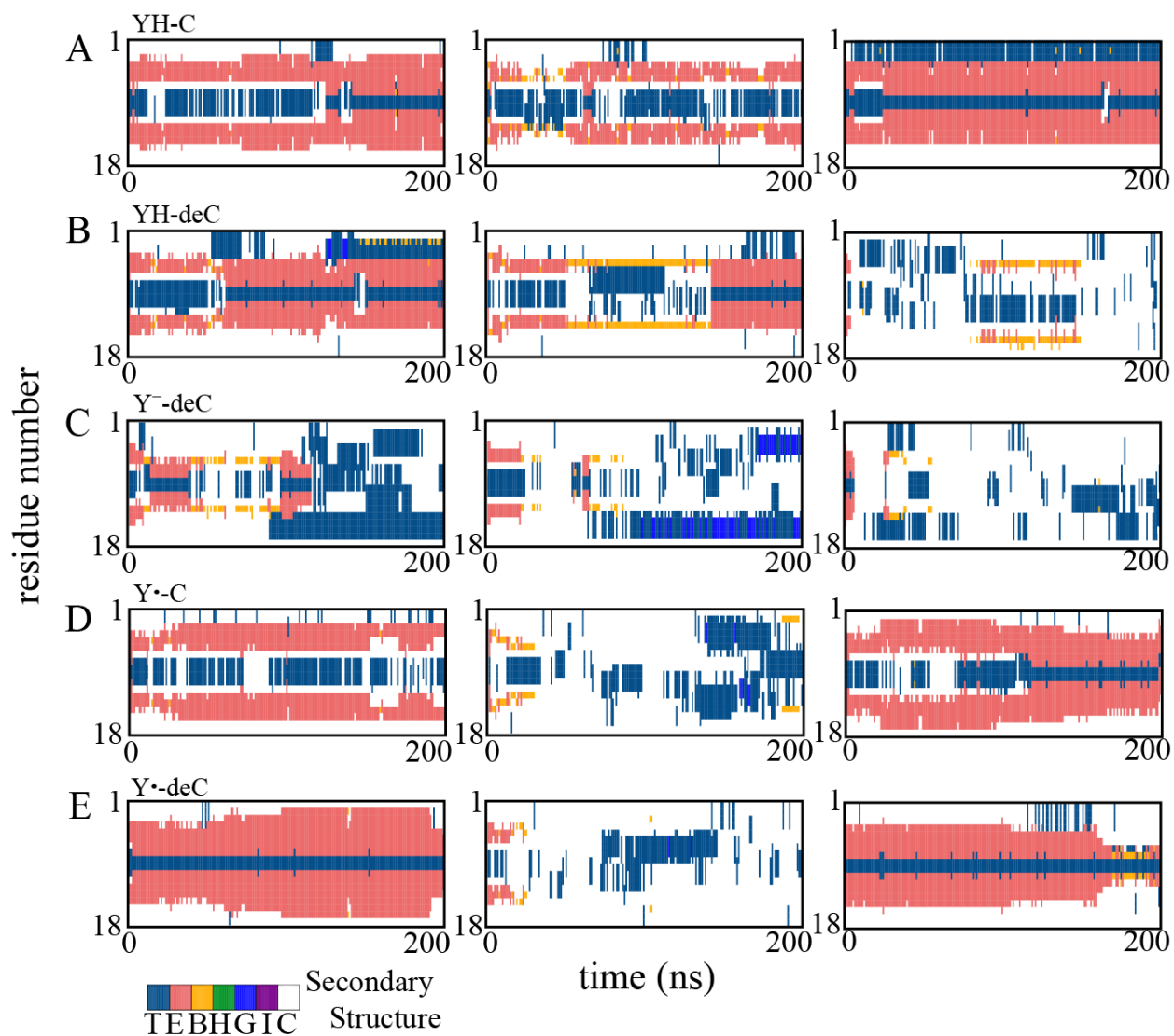


Figure S5. Time evolution of secondary structural assignment per residue derived from molecular dynamics simulations of Peptide O in different charge states of Y5 and C14 (Table S1). The results of three simulation runs are shown. The legend uses DSSP classification: T is β turn, E is β sheet, B is β bridge, H is α helix, G is 3_{10} helix, I is π helix, and C is unstructured coil.

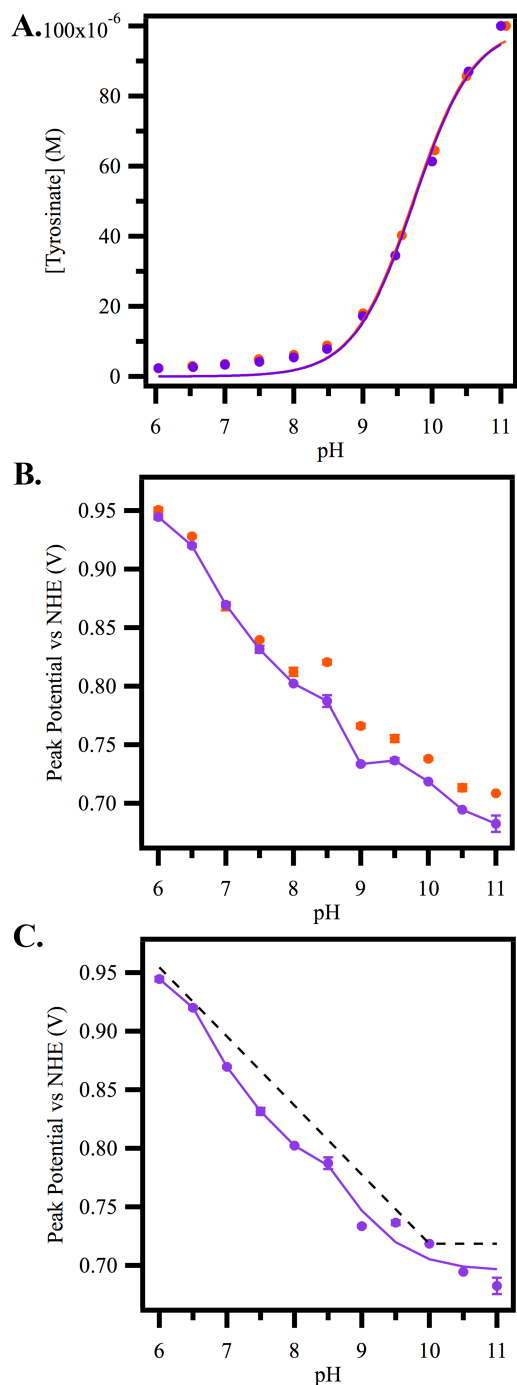


Figure S6. (A) UV-visible titration of the tyrosinate absorption band in Peptide O (purple) and Peptide A^{1,2} (orange) and (B) electrochemical titration of Peptide A (orange) and Peptide O (purple), using DPV. The peptide concentration was 100 μ M, and the buffer contained 200 mM KCl, and either 5 mM MES (pH 6 - 6.5), HEPES (pH 7 – pH 8), or borate/NaOH (pH 8.5 – pH 11). In (A), the superimposed line is a fit to the Henderson-Hasselbach equation using a pK_a of 9.7. In (B), the superimposed line connects the Peptide O data points. In (C), the Peptide O data is repeated from Panel B and compared to predictions for tyrosine. The dashed line shows the

function expected for the oxidation of tyrosine, assigning a pK_a of 9.7, a slope of 59 mV/pH unit, and a measured potential at pH 10 of 719 mV. On other hand, the solid superimposed line, which represents the Peptide O data, was predicted through the use of a more complex Nernst equation (see below), modified to represent the contribution from three proton transfer reactions.^{1,2} The parameters were: pK_a values in the reduced, singlet state of 9.7, 9.0, and 3.2 and pK_a values in the radical, oxidized state of 0, 6.0, and 6.9. S was 0.048; E was 1.13 V. The pK_a of 9.7 is assigned to tyrosine. Tyrosyl radical has a pK_a value below zero,^{1,2} and does not contribute in this pH range. The pK_a values of 9 and 6.9 are assigned to cysteine 14 in Peptide O. The pK_a values of 3.2 and 6.0 are assigned to aspartate. A perturbation of an aspartate pK_a was reported previously in Peptide A,^{1,2} and the pK_a shift was assigned as a shift from 3 (reduced) to 6 (oxidized). In (A, B, and C), experiments were conducted in triplicate, and the mean and standard deviation are plotted.

Equation:

$$f(\text{pH}) = E - S \cdot \log\left(\frac{((10^{-\text{pH}})^3) + (((10^{-\text{pH}})^2) \cdot (10^{-\text{pkox1}})) + ((10^{-\text{pH}}) \cdot (10^{-\text{pkox1}}) \cdot (10^{-\text{pkox2}})) + ((10^{-\text{pkox1}}) \cdot (10^{-\text{pkox2}}) \cdot (10^{-\text{pkox3}}))}{((10^{-\text{pH}})^3) + (((10^{-\text{pH}})^2) \cdot (10^{-\text{pkred1}})) + ((10^{-\text{pH}}) \cdot (10^{-\text{pkred1}}) \cdot (10^{-\text{pkred2}})) + ((10^{-\text{pkred1}}) \cdot (10^{-\text{pkred2}}) \cdot (10^{-\text{pkred3}}))}\right)$$

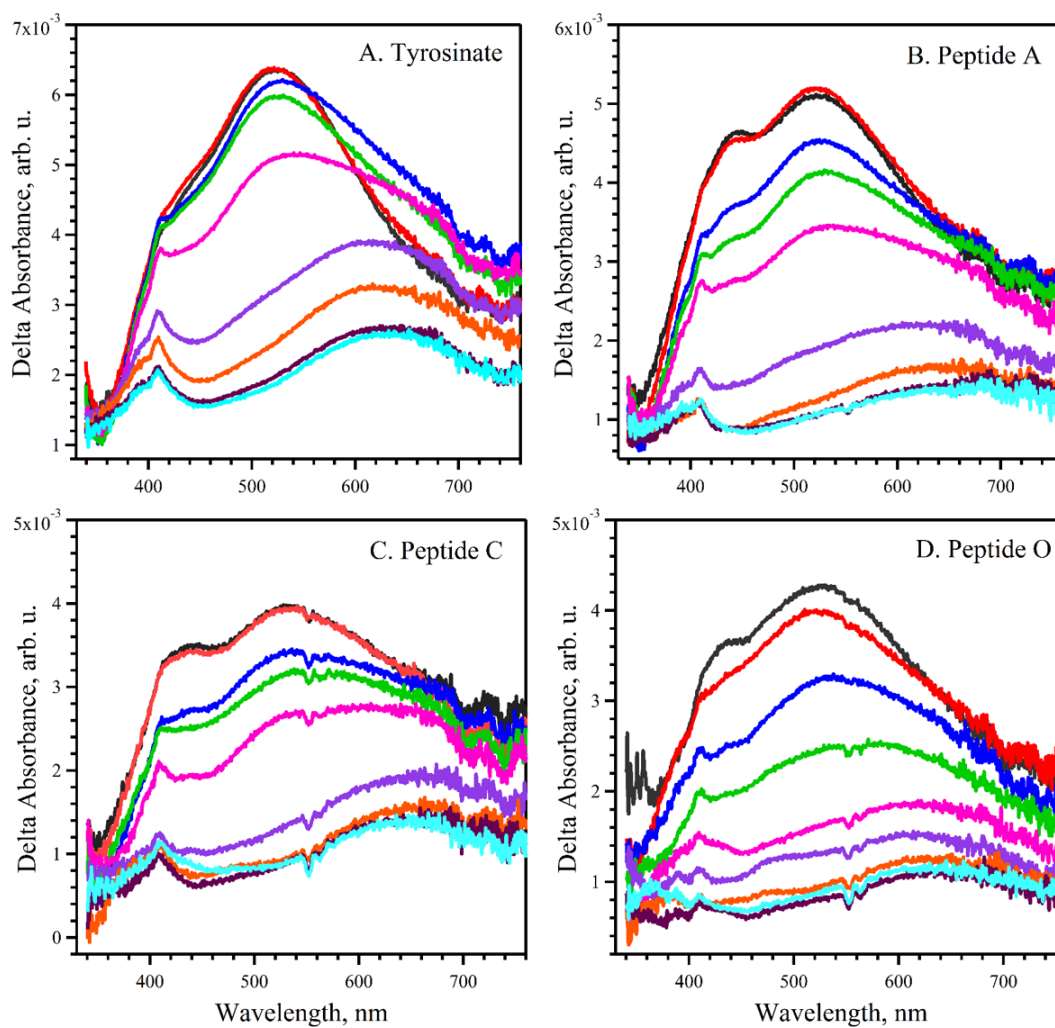


Figure S7. TRAS derived after a 280 nm photolysis pulse to tyrosinate (A), Peptide A (B), Peptide C (C) and Peptide O (D) at pD 11. Spectra were obtained at 2 (black), 3 (red), 10 (blue), 15 (green), 30 (pink), 100 (violet), 500 (orange), 1500 (purple) and 2000 ps (cyan). The spectra were averaged from at least three independent measurements. Analyte concentration, 1 mM; buffer, 5 mM borate-NaOD.

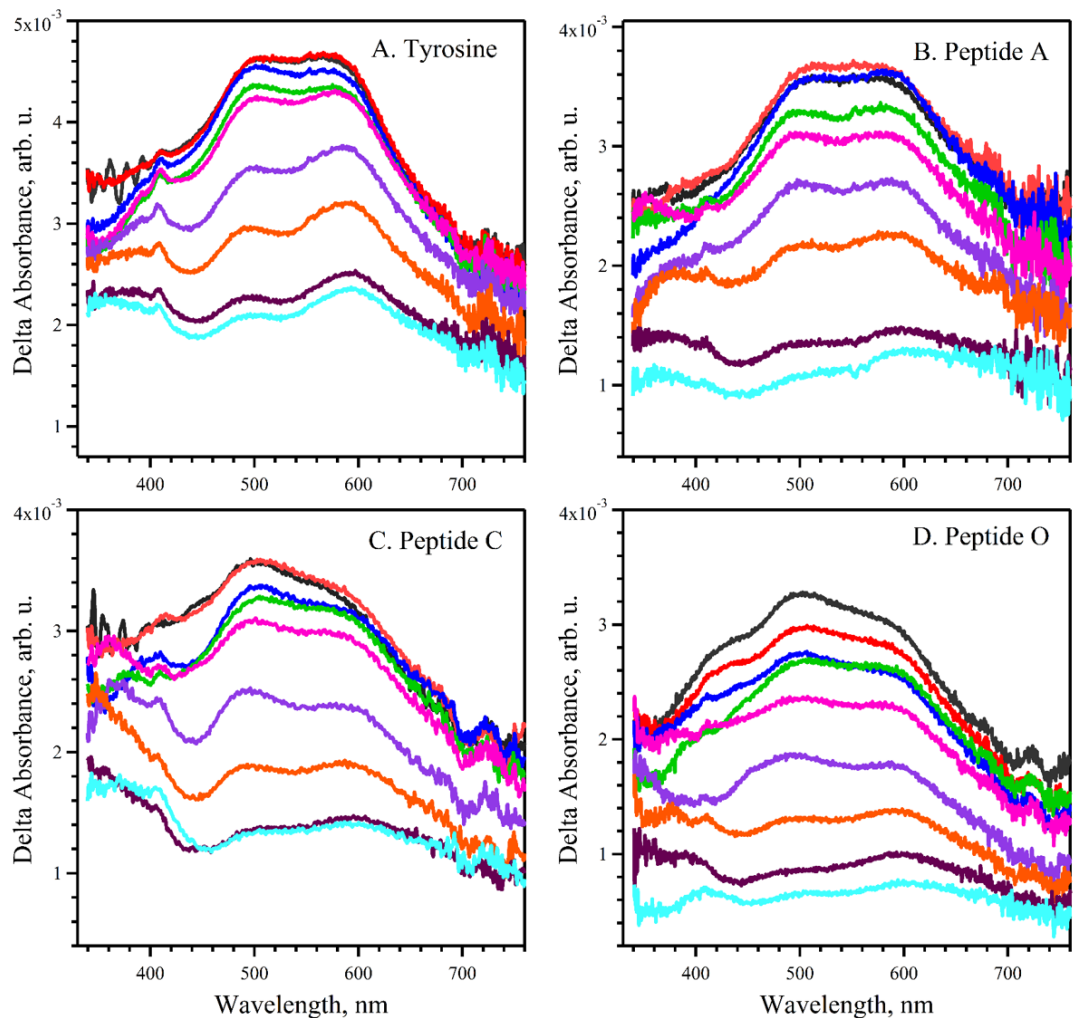


Figure S8. TRAS derived after a 280 nm photolysis pulse to tyrosine (A), Peptide A (B), Peptide C (C) and Peptide O (D) at pD 9. Spectra were obtained at 2 (black), 3 (red), 10 (blue), 15 (green), 30 (pink), 100 (violet), 500 (orange), 1500 (purple) and 2000 ps (cyan). The spectra were averaged from at least three independent measurements. Analyte concentration, 1 mM; buffer, 5 mM borate-NaOD.

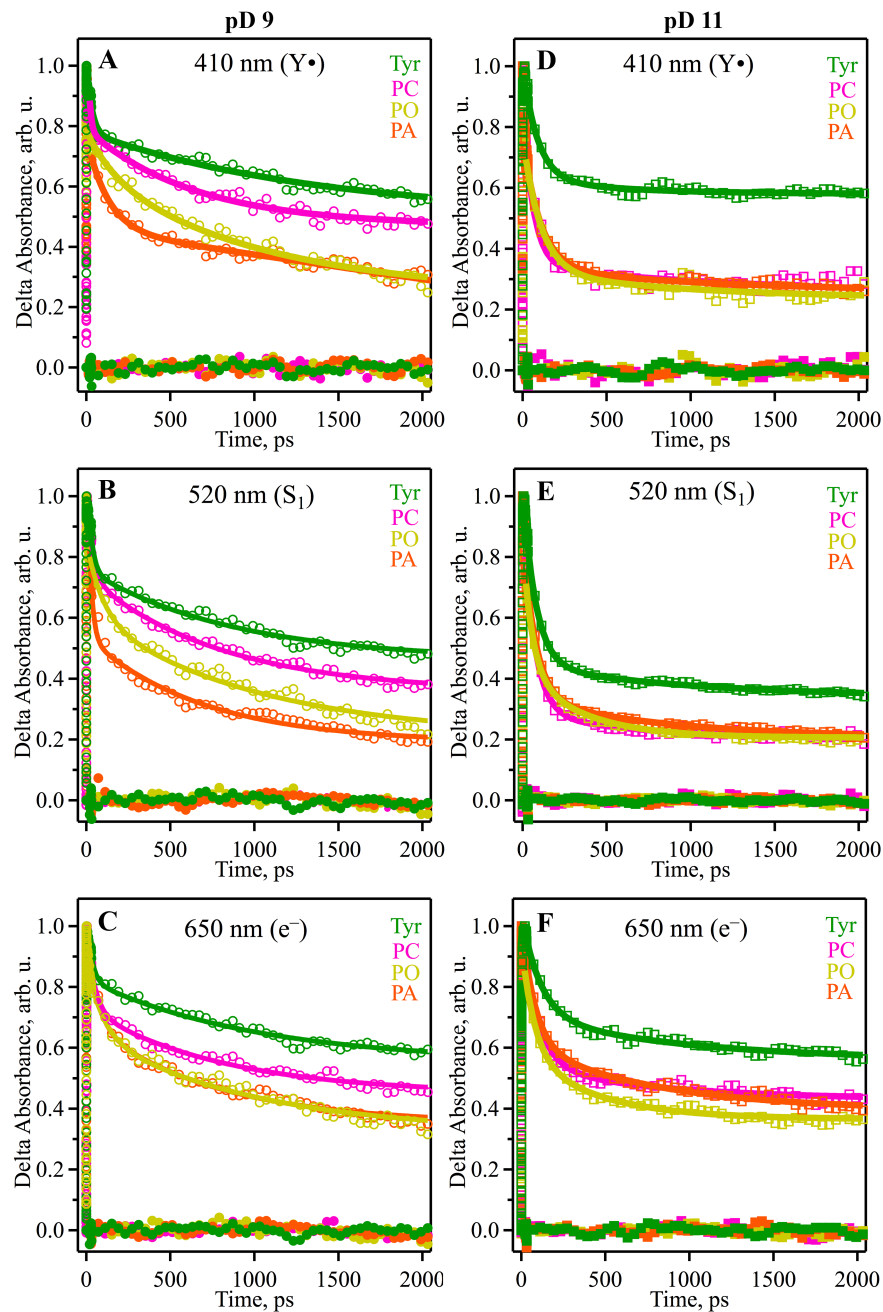


Figure S9. Decay kinetics as derived from TRAS acquired for tyrosine/tyrosinate and peptides in pD 9 (A-C) and pD 11 (D-F) buffer. Data were recorded after 280-nm photolysis at pD 9 (A-C, open circles) or pD 11 (D-F, open squares). Samples were tyrosine/tyrosinate (green), Peptide A (orange), Peptide C (pink) and Peptide O (yellow). In each sample, the absorption of the neutral tyrosyl radical was monitored at 410 nm (A, D), the absorption of the S_1 excited state was monitored at 520 nm (B, E), and absorption from the solvated electron was monitored at 650 nm (C, F). Double exponential fits (starting from 20 ps) are superimposed as the solid lines, and the closed circles/squares are the corresponding residuals. Fitting parameters are presented in Table S2. The data were averaged from at least two independent measurements. The averaged data were normalized with respect to the maximum absorbance, which occurred at ~ 3 – 4 ps at 410 and 520 nm and at ~ 10 – 15 ps at 650 nm. Analyte concentration, 1 mM; buffer, 5 mM borate-NaOD.